

See discussions, stats, and author profiles for this publication at: <https://www.researchgate.net/publication/231528853>

Modeling the Photosynthetic Water Oxidation Complex: Activation of Water by Controlled Deprotonation and Incorporation into a Tetranuclear Manganese Complex

ARTICLE in JOURNAL OF THE AMERICAN CHEMICAL SOCIETY · MAY 1998

Impact Factor: 12.11 · DOI: 10.1021/ja9730573

CITATIONS

37

READS

3

6 AUTHORS, INCLUDING:



Sheila Aubin

Gen-Probe

61 PUBLICATIONS 3,301 CITATIONS

SEE PROFILE



David Hendrickson

University of California, San Diego

599 PUBLICATIONS 26,556 CITATIONS

SEE PROFILE



George Christou

University of Florida

758 PUBLICATIONS 29,401 CITATIONS

SEE PROFILE

Modeling the Photosynthetic Water Oxidation Complex: Activation of Water by Controlled Deprotonation and Incorporation into a Tetranuclear Manganese Complex

Guillem Aromí,[†] Michael W. Wemple,[†] Sheila J. Aubin,[‡] Kirsten Folting,[†] David N. Hendrickson,^{*,‡} and George Christou^{*,†}

Department of Chemistry and Molecular Structure Center
Indiana University, Bloomington, Indiana 47405-4001
Department of Chemistry, 0358, University of California
at San Diego, La Jolla, California 92093-0358

Received September 2, 1997

Elucidating the structure and mechanism of action of the predominantly carboxylate-ligated, oxide-bridged Mn₄ cluster at the water oxidation center (WOC) of plants and cyanobacteria is of great current interest.^{1,2} This cluster binds, deprotonates, and oxidatively couples two H₂O molecules to yield O₂, but the precise details of this transformation are unclear. Recently, we have developed preparative methodology to the Mn^{III}Mn^{IV} complexes [Mn₄O₃X(O₂CMe)₃(dbm)₃] (X[−] = Cl[−], Br[−], PhCO₂[−], MeCO₂[−]; dbmH = dibenzoylmethane)³ containing the [Mn₄O₃] oxide-bridged trigonal pyramidal Mn₄ core that is one of the topologies consistent with recent EXAFS data on the native site,⁴ which has both short (~2.7 Å) and long (~3.3 Å) Mn...Mn separations. A major objective is to employ these model complexes to obtain structural and mechanistic insights into the interaction of the native cluster with its cofactors (Cl[−], Br[−], NO₃[−], etc.), inhibitors (F[−], NH₃, RNH₂, ROH), and substrate (H₂O);¹ we have shown, for example, that [Mn₄O₃(O₂CMe)₄(dbm)₃] (**1**) readily reacts with a F[−] source to give [Mn₄O₃F(O₂CMe)₃(dbm)₃].^{3c} Understanding the means by which a Mn₄ cluster binds, deprotonates, and oxidizes H₂O molecules is the primary objective, and we are attempting to use model complexes to achieve this in a stepwise fashion that might allow intermediates to be identified and thus provide insights into how such a transformation might proceed. In the present work, we report that **1** will spontaneously react with H₂O under mild, nonforcing conditions leading to deprotonation of the latter and its incorporation into the core. This reaction represents a controlled activation of H₂O and is proposed as a model system for the crucial first steps along the path to O₂ evolution.

The reactivity of **1** with H₂O and MeOH was conveniently monitored by ²H NMR spectroscopy using [Mn₄O₃(O₂CCD₃)₄(dbm)₃] (**1a**); this avoids the complicating presence of dbm resonances and gives sharper resonances than ¹H NMR spectroscopy. In addition to the signal for CHDCl₂ impurity, the spectrum of **1a** at room temperature shows two signals at 36.8 and 66.1 ppm in a 3:1 integration ratio from the μ₃-O₂CCD₃ and unique μ₃-O₂CCD₃ groups, respectively (Figure 1, top). Addition of distilled MeOH causes a decrease in these two signals and

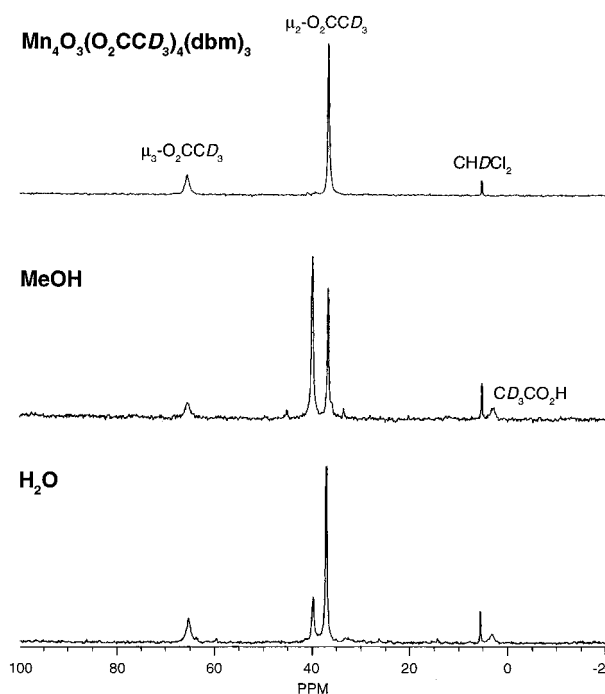
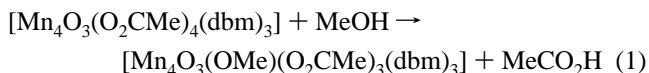


Figure 1. ²H NMR spectrum at ~23 °C of complex **1a** in CD₂Cl₂ (top); spectrum resulting from addition of 10 equiv of MeOH (middle); spectrum resulting from addition of an excess (immiscible) of H₂O (bottom).

appearance of free CD₃CO₂H at ~3 ppm and a new resonance at 39.7 ppm (Figure 1, middle). Addition of more MeOH causes an increase in the latter two signals at the expense of the former two. These data suggest a site-specific ligand substitution of the unique acetate group to give [Mn₄O₃(OMe)(O₂CCD₃)₃(dbm)₃] (**2a**). Similarly, addition of an excess of distilled H₂O (only sparingly miscible in CD₂Cl₂) causes analogous spectral changes with a new resonance appearing at 39.5 ppm (Figure 1, bottom), again suggesting displacement of the unique μ₃-CD₃CO₂[−] group and possible formation of [Mn₄O₃(OH)(O₂CCD₃)₃(dbm)₃] (**3a**). Firm identification of these two products followed from their bulk isolation and structural characterization.

Complex **1** was dissolved in CH₂Cl₂ containing ~300 equiv of MeOH, the solvent removed in vacuo, the cycle repeated, and the residue again dissolved in CH₂Cl₂/MeOH; the product was precipitated with Et₂O, filtered, and dried in vacuo to give [Mn₄O₃(OMe)(O₂CMe)₃(dbm)₃] (**2**) in ~50% yield (eq 1). With



the identity of **2** established,^{5,6} its reaction with H₂O was found to provide a more convenient route to **3**. Thus, **2** was twice treated to cycles of dissolution in CH₂Cl₂/MeCN (7:1) containing 30 equiv of H₂O, followed by precipitation of the solid with Et₂O. The final solid of [Mn₄O₃(OH)(O₂CMe)₃(dbm)₃] (**3**) was obtained in 55–60% yield (eq 2).⁷

(5) Dried solid analyzed as 2·1/4CH₂Cl₂. Anal. Calcd (found): C, 53.8 (53.8); H, 4.1 (4.0). Crystal data for 2·2CH₂Cl₂: monoclinic, *P*2₁/*c*, *a* = 14.278(5) Å, *b* = 15.108(6) Å, *c* = 27.500(12) Å, β = 100.51(2)°, *Z* = 4, *V* = 5832 Å³, *d*_{calc} = 1.498 g cm^{−3}, *T* = −171 °C; *R*(*F*) = 9.82 and *R*_w(*F*) = 8.77% using 5203 unique reflections with *F* > 3σ(*F*).

(6) Pure **2a** was made in a similar fashion from **1a**. The ²H NMR spectrum of **2a** exhibits only the 39.7 ppm resonance, confirming **2a** as the product of the methanolysis in Figure 1, middle.

(7) Pure **3a** was made in a similar fashion from **2a**. The ²H NMR spectrum of **3a** exhibits only the 39.5 ppm resonance, confirming **3a** as the product of the hydrolysis in Figure 1, bottom.

[†] Indiana University.

[‡] University of California at San Diego.

(1) (a) Debus, R. J. *Biochim. Biophys. Acta* **1992**, *1102*, 269. (b) *Manganese Redox Enzymes*; Pecoraro, V. L., Ed.; VCH Publishers: New York, 1992.

(2) (a) Ruettinger, W. F.; Dismukes, G. C. *Chem. Rev.* **1997**, *97*, 1. (b) Manchandra, R.; Brudvig, G. W.; Crabtree, R. *Coord. Chem. Rev.* **1995**, *144*, 1.

(3) (a) Wang, S.; Tsai, H.-L.; Folting, K.; Streib, W. E.; Hendrickson, D. N.; Christou, G. *Inorg. Chem.* **1996**, *35*, 7578. (b) Wang, S.; Tsai, H.-L.; Hagen, K. S.; Hendrickson, D. N.; Christou, G. *J. Am. Chem. Soc.* **1994**, *116*, 8376. (c) Wemple, M. W.; Adams, D. M.; Folting, K.; Hendrickson, D. N.; Christou, G. *J. Am. Chem. Soc.* **1995**, *117*, 7275.

(4) (a) DeRose, V. J.; Mukerji, I.; Latimer, M. J.; Yachandra, V. K.; Sauer, K.; Klein, M. P. *J. Am. Chem. Soc.* **1994**, *116*, 5239 and references therein. (b) Yachandra, V. K.; DeRose, V. J.; Latimer, M. J.; Mukerji, I.; Sauer, K.; Klein, M. P. *Science* **1993**, *260*, 675.

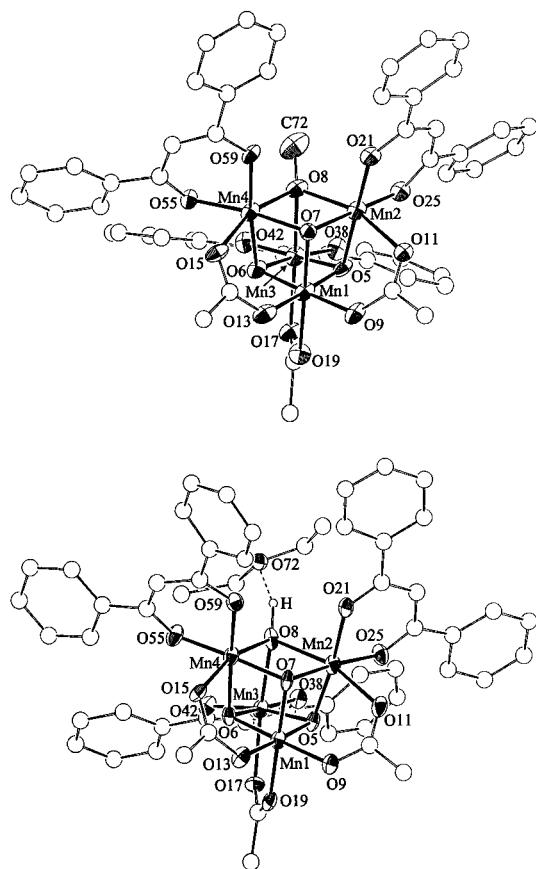
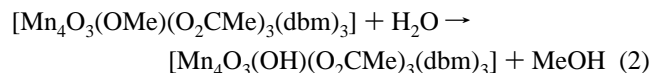


Figure 2. ORTEP representations of complexes **2** (top) and **3** (bottom) at the 50% probability level.

Table 1. Comparison of $[\text{Mn}_4\text{O}_3\text{X}]^{6+}$ Core Distances in Complexes **1–3**^{a–c}

	1	2	3
Mn ^{III} ...Mn ^{IV}	2.799(12)	2.798(6)	2.789(2)
Mn ^{III} ...Mn ^{III}	3.201(12)	3.132(26)	3.122(17)
Mn ^{III} –O _X	2.299(21)	2.182(23)	2.215(39)
Mn ^{III} –O _b	1.933(21)	1.936(23)	1.930(25)
Mn ^{IV} –O _b	1.867(9)	1.862(9)	1.862(12)

^a Averaged using C_{3v} virtual symmetry. ^b Numbers in parentheses are the greatest deviations of single values from the mean. ^c Mn(1) is Mn^{IV}; Mn(2), Mn(3), and Mn(4) are Mn^{III}; O_X = O of μ_3 -MeCO₂[–], MeO[–], or HO[–]; O_b = μ_3 -O^{2–} ions.



The structures of **2**⁵ and **3**⁸ (Figure 2) show great similarity to that of **1** except that the μ_3 -O₂CMe[–] is replaced by μ_3 -OMe[–] or OH[–] groups: in each case there is a Mn^{III}₃Mn^{IV} trigonal pyramid whose Mn^{III}₃ basal face is capped by a μ_3 -X[–] (X[–] = O₂CMe[–], OMe[–], OH[–]) group and its other faces by μ_3 -O^{2–} to give a highly distorted cubane $[\text{Mn}_4\text{O}_3\text{X}]^{6+}$ core. Interatomic distances (Table 1) confirm retention of both “short” (~2.8 Å) and “long” (3.1–3.2 Å) Mn...Mn separations in **2** and **3**; indeed, variation of X[–] causes almost insignificant changes to the structure of the core. Note that the $[\text{Mn}_4\text{O}_3(\text{OH})]^{6+}$ core of **3** is different from the more symmetric $[\text{Mn}_4\text{O}_4]^{6+}$ cubane core of $[\text{Mn}_4\text{O}_4(\text{O}_2\text{PPh}_2)_6]$ where all Mn...Mn separations are in the range 2.904–2.954 Å.⁹ The presence of hydrogen bonding in **3** between the μ_3 -OH[–] and an

Et₂O group (O...O = 2.951(16) Å) confirms the protonated nature of O(8). The X[–] groups in **1–3** lie on the three Mn^{III} Jahn–Teller elongation axes, and the resulting enhanced lability undoubtedly facilitates the site-specific substitution at this position. The process described in eq 1 is driven by the large excess (~300 equiv) of MeOH and the resulting shorter, stronger Mn^{III}–O_X bonds (table) even though the acidity of MeOH (pK_a = 15.5) is much less than MeCO₂H (4.8). The conversion in eq 2 is favored by the relative acidity of MeOH (pK_a = 15.5) versus H₂O (pK_a = 14) and such a large excess of H₂O is not necessary. We currently believe the substitutions occur via an intermediate whereby the μ_3 -X[–] (X[–] = MeCO₂[–] or MeO[–]) group becomes μ_2 -X[–] as the incoming group binds to one Mn^{III} site, followed by loss of XH as the new group is deprotonated and adopts a μ_3 mode.

Magnetic susceptibility data (2.00–300 K) on powdered samples of **2** and **3** were fit to the appropriate theoretical χ_m vs T expression for a C_{3v} symmetry Mn^{III}₃Mn^{IV} unit,^{3a,10} and the fitting parameters, in the format (J_{34} , J_{33} , g), were –31.8 cm^{–1}, +9.6 cm^{–1}, and 1.92 for **2** and –32.7 cm^{–1}, +11.9 cm^{–1}, and 2.02 for **3**. These values are very similar to those for **1** (–33.9 cm^{–1}, +5.4 cm^{–1}, and 1.94) and other $[\text{Mn}_4\text{O}_3\text{X}]$ (X[–] = Cl[–], Br[–], F[–]) complexes.^{3,10} Complexes **1–3** thus all have $S = 9/2$ ground states.

Complexes **1–3** display quasi-reversible one-electron reductions at 0.39, 0.16, and 0.16 V vs SCE, respectively, when examined by DPV and CV in CH₂Cl₂ and quasi-reversible oxidations at 1.55, 1.22, and 1.26 V. These changes with X[–] are consistent with the relative basicities of the latter as gauged by the above pK_a values and show that HO[–] and MeO[–] facilitate access to a higher oxidation state compared with MeCO₂[–]. The conversion of free H₂O into a bound OH[–] in **3** without change to the Mn₄O₃ core and via H⁺ transfer to a MeCO₂[–] or MeO[–] leaving group could parallel a similar transformation following (or accompanying) a S_n-to-S_{n+1} oxidation in the WOC, where according to recent theories both the electron and H⁺ transfers are to the Y_z tyrosine radical.^{11,12} The hydrogen-bonded Et₂O group may also be considered a model of how a second H₂O molecule could interact with the OH[–] to give a $[\text{H}_2\text{O} \cdots \text{HO}^-]$ pair poised for subsequent multiple deprotonations and oxidative coupling to form O₂;¹³ such a system would also be consistent with data showing both a slowly and rapidly exchanging substrate molecule at the native site.¹⁴ Current studies thus include isolation of **1** (or related species) at the 4Mn^{III} oxidation level to study H₂O binding and concomitant oxidation/deprotonation steps and deprotonation of **3** either alone or as a consequence of an oxidation to the 2Mn^{III}, 2Mn^{IV} level.

Acknowledgment. This work was funded by NIH Grants GM 39083 (G.C.) and HL 13652 (D.N.H.).

Supporting Information Available: Data collection and refinement details and listings of atomic coordinates and thermal parameters for complexes **2** and **3** and fitting of $\chi_m T$ vs T data for **2** and **3** (46 pages, print/PDF). See any current masthead page for ordering information and Web access instructions.

JA9730573

(9) Ruettinger, W. F.; Campana, C.; Dismukes, G. C. *J. Am. Chem. Soc.* **1997**, *119*, 6670.

(10) Hendrickson, D. N.; Christou, G.; Schmitt, E. A.; Libby, E.; Bashkin, J. S.; Wang, S.; Tsai, H.-L.; Vincent, J. B.; Boyd, P. D. W.; Huffman, J. C.; Folting, K.; Li, Q.; Streib, W. E. *J. Am. Chem. Soc.* **1992**, *114*, 2455.

(11) (a) Tang, X.-S.; Randall, D. W.; Force, D. A.; Diner, B. A.; Britt, R. D. *J. Am. Chem. Soc.* **1996**, *118*, 7638. (b) Gilchrist, M. L.; Ball, J. A.; Randall, D. W.; Britt, R. D. *Proc. Natl. Acad. Sci.* **1995**, *92*, 9545.

(12) (a) Tommos, C.; Tang, X.-S.; Warnecke, K.; Hoganson, C. W.; Styring, S.; McCracken, J.; Diner, B. A.; Babcock, G. T. *J. Am. Chem. Soc.* **1995**, *117*, 10325. (b) Hoganson, C. W.; Lydakis-Simantiris, X.; Tang, X.-S.; Tommos, C.; Warnecke, K.; Babcock, G. T.; Diner, B. A.; McCracken, J.; Styring, S. *Photosyn. Res.* **1995**, *46*, 177.

(13) We have, in fact, been able to crystallize **3** with the OH[–] hydrogen-bonded to two H₂O molecules instead of one Et₂O; however, the quality of the crystallographic data is currently very poor.

(14) Messinger, J.; Badger, M.; Wydrzynski, T. *Proc. Natl. Acad. Sci. U.S.A.* **1995**, *92*, 3209.

(8) Dried solid analyzed as **3**·Et₂O·1.7CH₂Cl₂. Anal. Calcd (found): C, 50.4 (50.4); H, 4.2 (4.2). Crystal data for **3**·0.9Et₂O·1.1CH₂Cl₂: monoclinic, $P2_1/c$, $a = 14.478(5)$ Å, $b = 14.910(5)$ Å, $c = 26.644(8)$ Å, $\beta = 101.00(2)^\circ$, $Z = 4$, $V = 5646$ Å³, $d_{\text{calc}} = 1.518$ g cm^{–3}, $T = -171$ °C; $R(F) = 7.84$ and $R_w(F) = 7.57\%$ using 4836 unique reflections with $F > 3\sigma(F)$.